Search for Muon Neutrino Disappearance in a Short-Baseline Accelerator Neutrino Beam

Yasuhiro Nakajima, for the SciBooNE Collaboration

Kyoto University Kitashirakawa-Oiwake-cho, Sakyo-ku, Kyoto 606-8502, Japan

Abstract

We report a search for muon neutrino disappearance in the Δm^2 region of $0.5-40$ eV^2 using data from both SciBooNE and MiniBooNE experiments. SciBooNE data provides a constraint on the neutrino flux, so that the sensitivity to ν_μ disappearance with both detectors is better than with just MiniBooNE alone. The preliminary sensitivity for a joint ν_μ disappearance search is presented.

1. Introduction

Neutrino oscillations have been observed and confirmed at mass splitting (Δm^2) of $\sim 10^{-5}$ eV^2 and $\sim 10^{-3}$ eV^2, called the "solar" and "atmospheric" regions, respectively. The observed mixing is consistent with three generations of neutrinos.

However, the LSND experiment observed an excess of $\overline{\nu}_e$ in a $\overline{\nu}_\mu$ beam, indicating a possible oscillation in the $\Delta m^2 \sim 1$ eV^2 region [1]. To explain LSND with oscillations requires more than three generations of neutrinos or other exotic physics beyond the Standard Model.

To test the oscillation at $\Delta m^2 \sim 1$ eV^2, the MiniBooNE experiment recently made searches for both ν_e appearance [2, 3] and ν_μ disappearance [4] in this parameter region. The experiment observed no significant ν_e appearance signal and ruled out as being due to 2-neutrino oscillations. However, the sensitivity of MiniBooNE-only ν_μ disappearance search was limited by the large flux and neutrino interaction cross-section uncertainties.

Here, we discuss an improved search for ν_μ disappearance using data from both the SciBooNE [5] and the MiniBooNE experiments, where SciBooNE detector is used to constrain flux and cross-section uncertainties.

2. Experimental Setup

2.1. Fermilab Booster Neutrino Beam

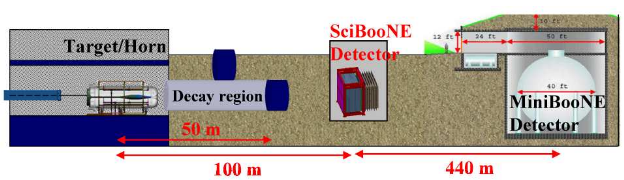

Fig. 1. The setup of SciBooNE and MiniBooNE experiments.

The experiments use the Booster Neutrino Beam (BNB) at Fermilab [6]. The primary proton beam, extracted with a kinetic energy of 8 GeV, strikes a 71 cm long, 1 cm diameter beryllium target. The mesons, primarily π^+, generated by the $p-$Be interactions are focused with a magnetic horn and decay in the following 50 m decay volume, producing an intense neutrino beam with the peak energy of $\sim$0.7 GeV. When the horn polarity is reversed, π^- are focused and hence a predominantly antineutrino beam is created.

2.2. SciBooNE Detector

The SciBooNE detector [5] is located 100 m downstream from the beryllium target.

The detector complex consists of three sub-detectors: a fully active fine grained scintillator tracking detector (SciBar), an electromagnetic calorimeter (EC) and a muon range detector (MRD).

The SciBar detector consists of 14,336 extruded plastic scintillator strips (CH), each with dimension of $1.3 \times 2.5 \times 300$ cm^3. The scintillators are arranged vertically and horizontally to construct a $3 \times 3 \times 1.7$ m^3 detector. The detector itself is the neutrino target and its fiducial volume is 10.6 tons.

The EC is installed downstream of the SciBar, and is made of scintillating fibers embedded in lead foil.

The MRD is located downstream of the EC in order to measure the momentum of muons up to 1.2 GeV/c using the muon range. It consists of 12 layers of 2"-thick iron plates sandwiched between layers of 6 mm-thick plastic scintillator planes.

The SciBooNE experiment ran from June 2007 until August 2008, collecting a total of 2.52×10^{20} Protons on Target (POT) for physics analysis; 0.99×10^{20} POT in neutrino mode and 1.53×10^{20} POT in antineutrino mode.

2.3. MiniBooNE Detector

The MiniBooNE detector [7] is located 440 m downstream from the SciBooNE detector. The detector is a 12 m diameter spherical tank filled with 800 tons of mineral oil (CH_2). The MiniBooNE experiment has been taking beam data since 2002, including the SciBooNE and MiniBooNE joint-run period. The collected number of POT after data quality cut in the neutrino mode is 5.579×10^{20} in addition to the data from the joint-run period.

3. ν_μ Disappearance Analysis

3.1. Analysis Overview

In this paper, we report only the neutrino data ($\nu_\mu \rightarrow \nu_x$) disappearance analysis. We search for muon neutrino disappearance by comparing neutrino fluxes at SciBooNE and MiniBooNE detectors.

The analysis is performed in the following three steps: (1) Neutrino flux measurement at SciBooNE, (2) Flux extrapolation to MiniBooNE, and (3) Oscillation fit.

At each step, systematic errors are estimated and propagated to the final prediction. The majority of the flux and cross-section uncertainties cancels since the neutrino interaction target in both detectors is effectively carbon, and the two detectors are on the same beam line.

We describe these steps in detail in the following sections.

3.2. Neutrino Flux Measurement at SciBooNE

Charged Current Event Selection

For the spectrum analysis at SciBooNE, we use inclusive ν_μ charged current (CC) interactions, whose signature is long muon tracks. First, we identify muons by selecting the longest track with energy deposit consistent with a minimum-ionizing particle. Second, we require the vertex of the track to be within the SciBar fiducial volume. The events are further divided into two subsamples based on the location of the muon track end points: a "SciBar-stopped" sample containing muons that have stopped inside the SciBar detector and a "MRD-stopped" sample with muons that have stopped in the MRD. These two samples each contain approximately 14k and 20k events with mean energies of 0.8 and 1.1 GeV, respectively.

Spectrum Fitting

The neutrino spectrum at SciBooNE is extracted by fitting muon momentum (P_μ) and muon angle (θ_μ) distributions from each sample.

We prepare MC templates for P_μ and θ_μ distributions for several true neutrino energy (E_ν) regions. The E_ν regions are divided by 250 MeV up to 1.25 GeV, and a single region is assigned for $E_\nu > 1.25$ GeV. Then, the scale factors for each E_ν region are determined to minimize the χ^2 between data and MC. Figure 2. shows the fit result. The systematic errors from SciBooNE detector response and neutrino cross-section models are estimated and shown in the plot.

Figure 3. is the P_μ and θ_μ distributions of SciBooNE's MRD-stopped sample, after applying scale factors obtained by the spectrum fitting. We confirm the MC distributions agrees well to data after fitting.

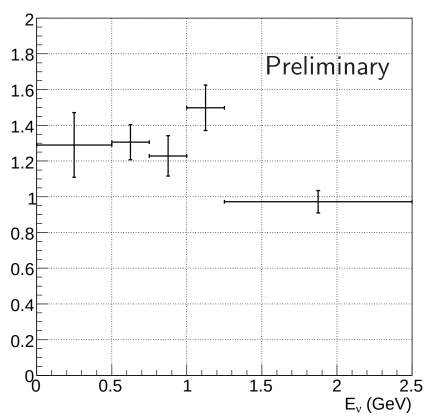

Fig. 2. Scale factors obtained by SciBooNE spectrum fitting. The error bars show the sum of SciBooNE statistical and systematic uncertainties.

3.3. Flux Extrapolation to MiniBooNE

MiniBooNE Event Selection

We select events in MiniBooNE by requiring single muon and its decay electron. Neutrino energy is reconstructed from muon kinematics by assuming CC Quasi Elastic (CCQE) interaction ($\nu_\mu n \to \mu^- p$):

$$E_\nu^{Rec} = \frac{2(M_n - E_B)E_\mu - (E_B^2 - 2M_nE_B + \Delta M + M_\mu^2)}{2[(M_n - E_B) - E_\mu + p_\mu \cos\theta_\mu]},$$

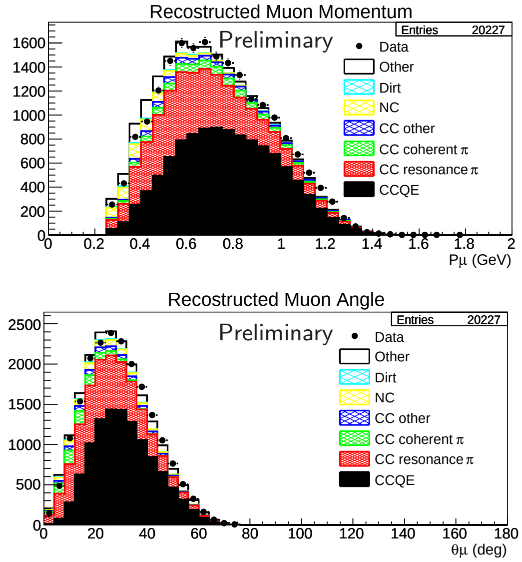

Fig. 3. Distribution of reconstructed muon momentum (top) and muon angle (bottom) for the MRD-stopped sample. The dots show the data, and histograms show the MC prediction with the contributions from neutrino interaction modes. The MC distributions are tuned by the E_ν scale factors obtained by the spectrum fit.

where $\Delta M = M_n^2 - M_p^2$; M indicate the muon, proton, or neutron mass with appropriate subscripts; E_B is the nucleon binding energy; E_μ is the reconstructed muon energy.

MiniBooNE E_ν^{Rec} prediction

To predict the E_ν^{Rec} distribution at MiniBooNE, we extrapolate the measured SciBooNE flux to MiniBooNE in two steps.

First, we apply MiniBooNE/SciBooNE flux ratio to make a prediction of the true neutrino energy distribution at MiniBooNE. Then, we smear the true neutrino energy prediction to the reconstructed neutrino energy.

Systematic uncertainties for the flux ratio is estimated by varying the cross-section and flux models. Additionally, the uncertainties of the smearing function, which convert true E_ν to E_ν^{Rec}, is estimated by varying the cross-section models.

Finally, we add MiniBooNE detector response error to the E_ν^{Rec} prediction.

The predicted MiniBooNE reconstructed neutrino energy distribution and its systematic uncertainties are shown in the Figure 4..

3.4. Oscillation Fit and Sensitivity

Fit Method

We test the oscillation hypothesis assuming the mixing between 2 neutrino flavors; ν_μ and ν_x. The $\nu_\mu \to \nu_x$ disappearance probability is given as

$$P(\nu_\mu \to \nu_x) = \sin^2 2\theta \sin^2(1.27\Delta m^2 L/E),$$

where θ is the mixing angle, $\Delta m^2[\mathrm{eV}^2]$ is the mass splitting between 2 flavors, L[km] is the distance traveled and E[GeV] is the neutrino energy.

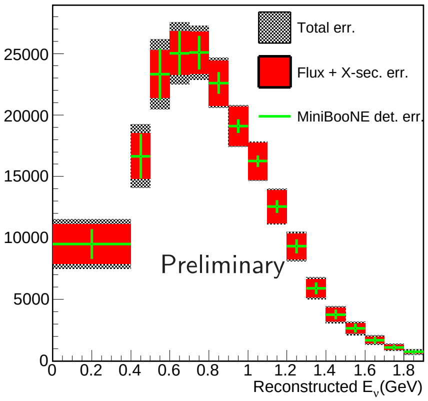

Fig. 4. Predicted MiniBooNE reconstructed neutrino energy distribution. MiniBooNE detector error, flux and cross-section uncertainty, and the total systematic uncertainty are separately shown.

We fit the MiniBooNE E_ν^{Rec} distribution to find the best fit parameter minimizing the χ^2 value:

$$\chi^2 = \sum_{i,j}^{16\ bins} (N_i^{data} - N_i^p) M_{ij}^{-1} (N_j^{data} - N_j^p),$$

where i, j denote E_ν^{Rec} bins, $N_{i,j}^{data}$ and $N_{i,j}^p$ denote observed and predicted number of events at each bin, respectively, and M_{ij} represents statistical and systematic uncertainties for the final E_ν^{Rec} prediction.

Then we define the allowed region by $\Delta\chi^2 = \chi^2(true) - \chi^2(best)$ values, where $\chi^2(true)$ is the χ^2 at the oscillation prediction being tested, and $\chi^2(best)$ is the smallest χ^2 value across the $(\Delta m^2, \sin^2 2\theta)$ plane.

To obtain the confidence level at each oscillation parameter point $(\Delta m^2, \sin^2 2\theta)$, we use Feldman-Cousins' method [8]. In this method, 1000 "fake-data" predictions are formed, using random draws of the statistical and systematic uncertainties and some underlying oscillation hypothesis. Then, each fake-data is fit to obtain the relation between the $\Delta\chi^2$ values and the corresponding probabilities. This process is repeated for each pair of $(\Delta m^2, \sin^2 2\theta)$ true oscillation parameter being tested.

Expected Limit

The sensitivity is defined as the average of limits obtained from fake experiments with null underlying oscillation.

Figure 5. shows the 90% CL. sensitivity for the ν_μ disappearance. The expected $\pm 1\sigma$ band is also shown in the plot. The expected sensitivity directly supersedes the MiniBooNE only ν_μ disappearance result, as substantial flux and cross section uncertainties have been reduced.

4. Summary and Prospects

We present SciBooNE-MiniBooNE joint analysis of a search for ν_μ disappearance in a accelerator neutrino beam. The analysis is sensitive to the oscillation at the Δm^2 region of $0.5 - 40$ eV^2. The sensitivity to ν_μ disappearance has been improved relative to the MiniBooNE shape-only analysis, with results to be released soon. In addition, a joint anti-neutrino oscillation analysis will be performed using the anti-neutrino data set.

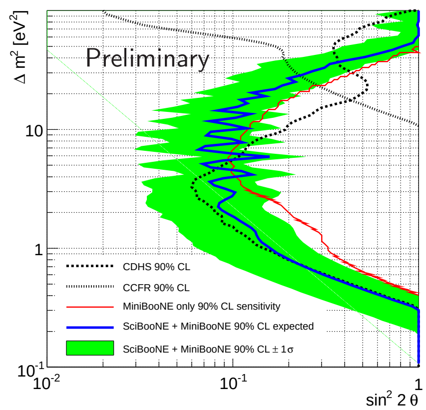

Fig. 5. The expected sensitivity for ν_μ disappearance. The dotted curve shows the 90% CL limits from CDHS [9] and CCFR [10] experiments. The thin solid curve is the MiniBooNE-only 90% CL sensitivity. The thick solid curve and the filled region are the 90% CL sensitivity and $\pm 1\sigma$ band from SciBooNE-MiniBooNE joint analysis, respectively.

5. Acknowledgements

SciBooNE collaboration gratefully acknowledges the support from various grants and contracts from the Department of Energy (U.S.), the National Science Foundation (U.S.), the MEXT (Japan), the INFN (Italy) the Ministry of Education and Science and CSIC (Spain), and the STFC (UK). We thank MiniBooNE collaboration for various informations and simulation outputs. The author was supported by Japan Society for the Promotion of Science, and by the Grant-in-Aid for the Global COE Program "The Next Generation of Physics, Spun from Universality and Emergence" from the MEXT of Japan.

References

[1] A. Aguilar et al., Phys. Rev. D64 (2001) 112007.
[2] A. A. Aguilar-Arevalo et al., Phys. Rev. Lett. 98 (2007) 23180.
[3] A. A. Aguilar-Arevalo et al. Phys. Rev. Lett. 103 (2009) 111801.
[4] A. A. Aguilar-Arevalo et al., Phys. Rev. Lett. 103 (2009) 061802.
[5] K. Hiraide et al., Phys. Rev. D78 (2008) 112004.
[6] A. A. Aguilar-Arevalo et al., Phys. Rev. D79 (2009) 072002.
[7] A. A. Aguilar-Arevalo et al., Nucl. Instrum. Meth. A599 (2009) 28.
[8] G. J. Feldman and R. D. Cousins., Phys. Rev. D57 (1998) 3873.
[9] F. Dydak et al., Phys. Lett. B134 (1984) 281.
[10] I. E. Stockdale et al., Phys. Rev. Lett. 52 (1984) 1384.